

4. The Solenoid Magnet and Flux Return

4.1. Overview

The *BABAR* magnet system consists of a superconducting solenoid [19], a segmented flux return and a field compensating or *bucking coil*. This system provides the magnetic field which enables charged particle momentum measurement, serves as the hadron absorber for hadron/muon separation, and provides the overall structure and support for the detector components. Figures 1 and 2 show key components of the *BABAR* magnet system and some of the nearby PEP-II magnets.

The magnet coil cryostat is mounted inside the hexagonal barrel flux return by four brackets on each end. The flux return end doors are each split vertically and mounted on skids that rest on the floor. To permit access to the inner detector, the doors can be raised and moved on rollers. At the interface between the barrel and the end doors, approximately 60% of the area is occupied by structural steel and filler plates; the remaining space is reserved for cables and utilities from the inner detectors. A vertical, triangular chase cut into the backward *end doors* contains the cryostat chimney. Table 4 lists the principal parameters of the magnet system. The total weight of the flux return is approximately 870 metric tons.

To optimize the detector acceptance for unequal beam energies, the center of the *BABAR* detector is offset by 370 mm in the electron beam direction. The principal component of the magnetic field, B_z , lies along the $+z$ axis; this is also the approximate direction of the electron beam. The backward end door is tailored to accommodate the DIRC bar boxes and to allow access to the drift chamber electronics. Both ends allow space and adequate shielding for the PEP-II quadrupoles.

4.2. Magnetic Field Requirements and Design

4.2.1. Field Requirements

A solenoid magnetic field of 1.5 T was specified in order to achieve the desired momentum resolution for charged particles. To simplify track finding and fast and accurate track fitting, the magnitude of the magnetic field within the track-

Table 4
Magnet Parameters

Field Parameters		
Central Field	1.5	T
Max. Radial Field at Q1 and $r = 200$ mm	<0.25	T
Leakage into PEP-II	<0.01	T
Stored Energy	27	MJ
Steel Parameters		
Overall Barrel Length	4050	mm
Overall Door Thickness (incl. gaps for RPCs)	1149	mm
Overall Height	6545	mm
Plates in Barrel	18	
9	20	mm
4	30	mm
3	50	mm
2	100	mm
Plates in Each Door	18	
9	20	mm
4	30	mm
4	50	mm
1	100	mm
Main Coil Parameters		
Mean Diameter of Current Sheet	3060	mm
Current Sheet Length	3513	mm
Number of layers	2	
Operating Current	4596	A
Conductor Current Density	1.2	kA/mm ²
Inductance	2.57	H
Bucking Coil Parameters		
Inner Diameter	1906	mm
Operating Current	200	A
Number of Turns	140	
Cryostat Parameters		
Inner Diameter	1420	mm
Radial Thickness	350	mm
Total Length	3850	mm
Total Material (Al)	~ 126	mm

ing volume was required to be constant within a few percent.

The magnet was designed to minimize disturbance of operation of the PEP-II beam elements. The samarium-cobalt B1 dipole and Q1 quadrupole magnets are located inside the solenoid as shown in Figure 1. Although these magnets can sustain the high longitudinal field of 1.5 T, they cannot tolerate a large radial component. Specifically, the field cannot exceed 0.25 T at a radius $r = 200$ mm (assuming a linear dependence of B_r on r) without degrading their field properties due to partial demagnetization. The conventional iron quadrupoles Q2, Q4, and Q5 are exposed to the solenoid stray fields. To avoid excessive induced skew octupole components, the stray field leaking into these beam elements is required to be less than 0.01 T averaged over their apertures.

4.2.2. Field Design Considerations

Saturation of the steel near the coil and the gap between the coil and the steel leads to field non-uniformities. To control these non-uniformities, the current density of the coil is increased at the ends relative to the center by reducing the thickness of the aluminum stabilizer. While the requirements on the radial field component at Q1 inside the solenoid can be satisfied easily at the forward end, the shape of the backward plug had to be specifically designed to simultaneously control field uniformity and unwanted radial components.

Leakage of magnetic flux is a problem, in particular at the backward end. A bucking coil, mounted at the face of the backward door and surrounding the DIRC strong support tube, is designed to reduce the stray field to an acceptable level for the DIRC photomultipliers and the PEP-II quadrupoles.

4.2.3. Magnetic Modeling

Extensive calculations of the magnetic field were performed to develop the detailed design of the flux return, the solenoid coil, and the bucking coil. To crosscheck the results of these calculations the fields were modeled in detail in two and three dimensions using commercial software [20].

The shape of the hole in each end door was designed by optimizing various parameters, such as the minimum steel thickness in areas of saturation. The design of the hole in the forward door was particularly delicate because the highly saturated steel is very close to the Q2 quadrupole. The multiple *finger* design of the hole was chosen to control the saturation of the steel.

Most of the design work was performed in two dimensions, but some three dimensional calculations were necessary to assure the accuracy of modeling the transitions between the end doors and the barrel, the leakage of field into the PEP-II magnets, and the impact of that leakage on the multipole purity [21,22]. The computations of the leakage field were done for central field of 1.7 T instead of 1.5 T to provide some insurance against uncertainties in the modeling of complex steel shapes and the possible variations of the magnetic properties of the steel.

4.3. Steel Flux Return

4.3.1. Mechanical and Magnetic Forces

The magnet flux return supports the detector components on the inside, but this load is not a major issue. Far greater demands are placed on the structural design by the magnetic forces and the mechanical forces from a potential earthquake.

Magnetic forces are of three kinds. First, there is a symmetric magnetic force on the end doors which was taken into consideration in their design and construction. Second, there is an axial force on the solenoid due to the forward-backward asymmetry of the steel. Because the steel is highly saturated in places, the magnitude of the field asymmetry changes when the current is raised from zero, and there is no position of the solenoid at which the force remains zero at all currents. Because it is important that this axial force should not change sign, which could cause a quench, the superconducting solenoid was deliberately offset by 30 mm towards the forward door. This offset was chosen to accommodate a worst case scenario, including uncertainties in the calculation. Third, during a quench of the superconducting coil, eddy currents in conducting com-

ponents inside the magnetic volume could generate sizable forces. These forces were analyzed for components such as the endplates of the drift chamber and the electromagnetic calorimeter and were found not to be a problem.

4.3.2. Earthquake Considerations

Because SLAC is located in an earthquake zone, considerable attention has been given to protecting the detector against severe damage from such an event. The entire detector is supported on four earthquake isolators, one at each corner, which limit the component acceleration in the horizontal plane to 0.4 g. However, these isolators offer no protection in the vertical direction. Vertical ground accelerations of 0.6 g are considered credible and actual component accelerations may be considerably larger due to resonances. By taking into account resonant frequencies and the expected frequency spectra of earthquakes, the magnet and all detector components have been designed to survive these accelerations without serious damage. Because the magnet is isolated from the ground moving beneath it, worst case clearances to external components, *e.g.*, PEP-II components, are provided. It is expected that even during a major earthquake, damage would be modest.

4.3.3. Fabrication

The flux return was fabricated [23] from drawings prepared by the *BABAR* engineering team. A primary concern was the magnetic properties of the steel. The need for a high saturation field dictated the choice of a low carbon steel, specified by its chemical content (close to AISI 1006). The manufacturer supplied sample steel for critical magnetic measurements and approval. The availability of very large tools at the factory made it possible to machine the entire face of each end of the assembled barrel, thus assuring a good fit of the end doors. The entire flux return was assembled at the factory, measured mechanically, and inspected before disassembly for shipment.

4.4. Magnet Coils

The design of the superconducting solenoid is conservative and follows previous experience. The superconducting material is composed of

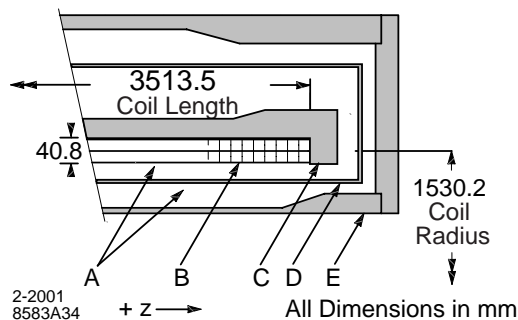


Figure 13. A portion of cryostat assembly. The forward end is shown. Legend: (A) evacuated spaces filled with IR-reflective insulator; (B) superconducting coil (2-layers); (C) aluminum support cylinder; (D) aluminum heat shield; (E) aluminum cryostat housing.

niobium-titanium (46.5% by weight Nb) filaments, each less than $40\ \mu\text{m}$ in diameter. These filaments are then wound into 0.8 mm strands, 16 of which are then formed into *Rutherford cable* measuring $1.4 \times 6.4\ \text{mm}$. The final conductor [24] consists of Rutherford cable co-extruded with pure aluminum stabilizer measuring $4.93 \times 20.0\ \text{mm}$ for use on the outer, high current density portion of the solenoid, and $8.49 \times 20.0\ \text{mm}$ for the central, lower current density portion. The conductor is covered in an insulating dry wrap fiberglass cloth which is vacuum impregnated with epoxy. The conductor has a total length of 10.3 km.

The solenoid is indirectly cooled to an operating point of 4.5K using a thermo-syphon technique. Liquid helium [25] is circulated in channels welded to the solenoid support cylinder. Liquid helium and cold gas circulate between the solenoid, its shields, the liquefier-refrigerator and a $4000\ \ell$ storage dewar via 60 m of coaxial, gas-screened, flexible transfer line. The solenoid coil and its cryostat were fabricated [26] to drawings prepared by the *BABAR* engineering team. Before shipment [27], the fully assembled solenoid was cooled to operating temperature and tested with currents of up to 1000 A, limited by coil forces in the absence of the iron flux return.

A portion of the cryostat assembly, containing the solenoid coil, its support cylinder and heat

shield, is shown in Figure 13.

To reduce the leakage fields into the PEP-II components and the DIRC photomultipliers, an additional external bucking coil is installed [28]. This is a conventional water cooled copper coil consisting of ten layers. Although the nominal operating current is 200 A, a current of up to 575 A is attainable, if needed, to demagnetize the DIRC shield.

To optimally control the stray fields and avoid a magnetization of the DIRC magnetic shield, the currents in the solenoid and the bucking coil are ramped together under computer control. High precision transducers are used to measure the currents and provide the feedback signals to the power supplies. The values of the currents are recorded in the *BABAR* database.

4.5. Magnetic Field Map

The goal of the magnetic field mapping and subsequent corrections was to determine the magnetic field in the tracking volume to a precision of 0.2 mT.

4.5.1. Mapping Procedure

A field mapping device was built specifically for the *BABAR* magnet based on a design concept developed at Fermilab [29]. The magnetic field sensors were mounted on a *propeller* at the end of a long cantilevered spindle which reached through the hole in the forward end door. The spindle in turn rode on a carriage which moved on precision-aligned rails. The propeller rotated to sample the magnetic volume in ϕ , and the carriage moved along its axis to cover z . Measurements were obtained from five sets of B_r and B_z and two B_ϕ Hall probes, all of which were mounted on a plate at different radial positions. This plate was attached to the propeller and its position could be changed to cover the desired range in the radial distance r from the axis. Precision optical alignment tools were used to determine the position of the sensors transverse to the z -axis.

The B_r and B_z probes were two-element devices with a short-term (few month) precision of 0.01%, the B_ϕ probes were single element devices with a precision of 0.1% [30]. In addition to the Hall probes, an NMR probe [31] was mounted at

a radius of 89 mm on the propeller to provide a very precise field reference near the z -axis as a function of z for $|z| < 1000$ mm, where $z = 0$ at the magnet center. The NMR measurements set the absolute scale of the magnetic field.

The magnetic field was mapped at the nominal central operating field of 1.5 T, as well as at 1.0 T. Measurements were recorded in 100 mm intervals from -1800 to $+1800$ mm in z , and in 24 azimuthal positions spaced by 15° for each of three different radial positions of the Hall probe plate. Thus for each z and ϕ position, the components B_r and B_z were measured at 13 distinct radii from 130 mm to 1255 mm and B_ϕ at six radii between 505 mm and 1180 mm.

The field map was parameterized in terms of a polynomial of degree up to 40 in r and z plus additional terms to account for expected perturbations [32]. The fit reproduced the measurements to within an average deviation of 0.2 mT throughout the tracking volume. The fitting procedure also served as a means of detecting and removing questionable measurements.

4.5.2. Perturbations to the Field Map

During the mapping process, the permanent magnet dipoles (B1) and quadrupoles (Q1) were not yet installed. Their presence inside the solenoid results in field perturbations of two kinds. The first is due to the fringe fields of the B1 and Q1 permanent magnets, and of the dipole and quadrupole trim coils mounted on Q1. The B1 field strength reaches a maximum of ~ 20 mT close to the surface of the B1 casing and decreases rapidly with increasing radius. The fields associated with the trim coils were measured and parameterized prior to installation; they are essentially dipole in character.

The second field perturbation is due to the permeability of the permanent magnet material. Sintered samarium-cobalt has a relative permeability of 1.11 to 1.13 in the z direction, and as a result the solenoid field is modified significantly. Probes between the B1 and Q1 magnets at a radius of about 190 mm measure the effect of the permeability. The field perturbation is obtained from a two-dimensional, finite element analysis which reproduces the r and z dependence of B_r ,

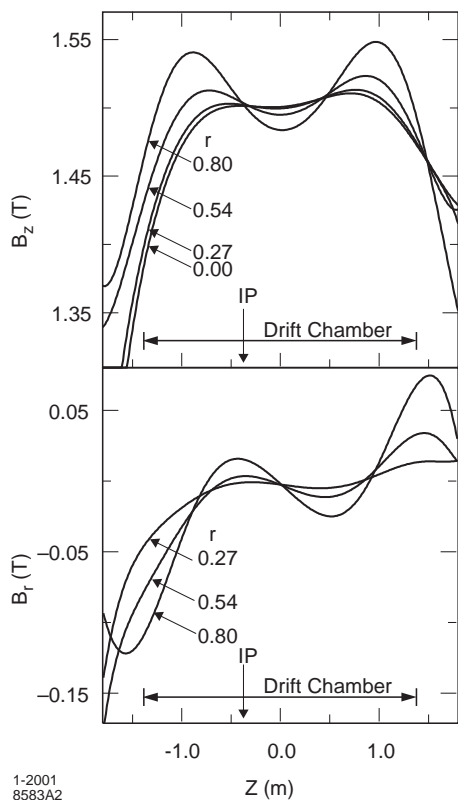


Figure 14. The magnetic field components B_z and B_r as a function of z for various radial distances r (in m). The extent of the DCH and the location of the interaction point (IP) are indicated.

and B_z . The induced magnetization increases B_z by about 9 mT at the interaction point; the effect decreases slowly with increasing radius.

4.5.3. Field Quality

To illustrate the quality of magnetic field, Figure 14 shows the field components B_z and B_r as a function of z for various radial distances r . In the tracking volume the field is very uniform, the B_ϕ component does not exceed 1 mT. The variation of the bend field, *i.e.*, the field transverse to the trajectory, along the path of a high momentum track is at most 2.5% from maximum to minimum within the tracking region, as shown in Figure 15.

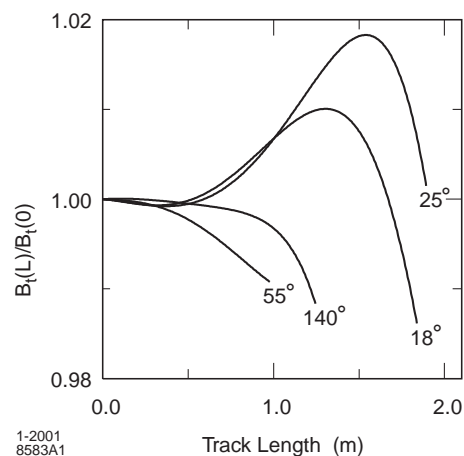


Figure 15. Relative magnitude of magnetic field transverse to a high momentum track as a function of track length from the IP for various polar angles (in degrees). The data are normalized to the field at the origin.

4.5.4. Field Computation

In order to reduce the computation of the magnetic field for track reconstruction and momentum determination, the field values averaged over azimuth are stored in a grid of r - z space points spanning the volume interior to the cryostat. Local values are obtained by interpolation. Within the volume of the SVT, a linear interpolation is performed in a 20 mm grid; elsewhere the interpolation is quadratic in a 50 mm grid. Azimuthal dependence is parameterized by means of a Fourier expansion at each r - z point. The Fourier coefficients at the point of interest are obtained by interpolation on the r - z grid, and the average field value is corrected using the resulting Fourier series.

4.6. Summary

Since its successful commissioning, the magnet system has performed without problems. There have been no spontaneous quenches of the superconducting solenoid. In the tracking region, the magnetic field meets specifications, both in magnitude and uniformity. The field compensation and magnetic shielding work well for the DIRC photomultiplier array and the external quadrupoles. Measurements indicate that the

bucking coil reduces the field at the face of Q2 from ~ 50 mT to ~ 1 mT [28], in agreement with calculations.